Relaxed equilibrium configurations to model fossil fields
I. A first family

V. Duez and S. Mathis

CEA/DSM/IRFU/SAp, CE Saclay, 91191 Gif-sur-Yvette Cedex, France; AIM, UMR 7158, CEA - CNRS - Université Paris 7, France
e-mail: [vincent.duez;stephane.mathis]@cea.fr

ABSTRACT

Context. The understanding of fossil fields' origin, topology, and stability is one of the corner stones of the stellar magnetism theory. On one hand, since they survive on secular time scales, they may modify the structure and the evolution of their host stars. On the other hand, they must have a complex stable structure since it has been demonstrated that the simplest purely poloidal or toroidal fields are unstable on dynamical time scales. In this context, the only stable configuration found today is the one resulting from a numerical simulation by Braithwaite and collaborators who studied the evolution of an initial stochastic magnetic field, which is found to relax on a mixed stable configuration (poloidal and toroidal) that seems to be in equilibrium and then diffuses.
Aims. We investigate an equilibrium field in a semi-analytical way. In this first article, we study the barotropic magnetohydrostatic equilibrium states.
Methods. The problem reduces to a Grad-Shafranov-like equation with arbitrary functions. These functions are constrained by deriving the lowest-energy equilibrium states for given invariants of the considered axisymmetric problem, in particular for a given helicity known to be one of the causes of such problems. These theoretical results were applied to realistic stellar cases, the solar radiative core and the envelope of an Ap star, and discussed. In both cases we assumed that the field is initially confined in the stellar radiation zone.
Results. The generalization of the force-free Taylor's relaxation states studied in laboratory experiments (in spheromaks) that become non force-free in the self-gravitating stellar case are obtained. The case of general baroclinic equilibrium states will be studied in Paper II.

Key words. magnetohydrodynamics (MHD) – plasmas – magnetic fields – stars: magnetic field

1. Introduction

Spectropolarimetry is currently exploring the stellar magnetism across the whole Hertzsprung-Russel diagram (Donati et al. 1997, 2006; Neiner 2007; Landstreet et al. 2008; Petit et al. 2008). Furthermore, helioseismology and asteroseismology are providing new constraints on internal transport processes occurring in stellar interiors (Turck-Chièze & Talon 2008; Aerts et al. 2008). In this context, even if standard stellar models explain the main features of stellar evolution, it is now crucial to go beyond this modelling to introduce dynamical processes such as magnetic field and rotation to investigate their effects on stellar structure and secular evolution (Maeder & Meynet 2000; Talon 2008). To achieve this aim, secular MHD transport equations have been derived to be introduced in stellar evolution codes. They coherently consider the interaction between differential rotation, turbulence, meridional circulation, and magnetic field (Spruit 2002; Maeder & Meynet 2004; Mathis & Zahn 2005), while nonlinear numerical simulations provide new insight into these mechanisms (Charbonneau & MacGregor 1993; Rudiger & Kitchatinov 1997; Garaud 2002; Brun & Zahn 2006). If we want to go further, the simplest modifications of static structural properties such as density, gravity, pressure, temperature, and luminosity induced by the magnetic field also have to be systematically quantified as a function of the field geometry and strength (Moss 1973; Mestel & Moss 1977; Lydon & Sofia 1995; Couvidat et al. 2003; Li et al. 2006; Duez et al. 2008; Li et al. 2009).

However, an infinity of possible magnetic configurations can be investigated because the different observation techniques only lead to indirect indications on the internal field topologies through the surface field properties they provide. Furthermore, since the simplest geometrical configurations, such as purely poloidal and purely toroidal fields are known to be unstable (Acheson 1978; Tayler 1973; Markey & Tayler 1973, 1974; Goossens & Veugelen 1978; Goossens & Tayler 1980; Goossens et al. 1981; Van Assche et al. 1982; Spruit 1999; Braithwaite 2006, 2007), the best candidates for stable geometries are mixed poloidal-toroidal fields (Wright 1973; Markey & Tayler 1974; Tayler 1980; Braithwaite 2009).

Therefore, it is necessary to track down possible stable magnetic configurations in stellar interiors so as to evaluate their effects on stellar structure and to use them as potential initial conditions for studying secular internal transport processes.

In this work, we thus revisit the pioneer works by Ferraro (1954), Mestel (1956), Prendergast (1956), and Woltjer (1960). Ferraro (1954) studied the equilibrium configurations of an incompressible star with a purely poloidal field. Prendergast (1956) (see also Chandrasekhar 1956a,b; Chandrasekhar & Prendergast 1956) then extended the model to take the toroidal field into account, by solving the magneto-hydrostatic equilibrium of incompressible spheres. The obtained configurations seem to be relevant to both the most recent numerical simulations that may explain fossil fields in early-type stars, white dwarfs, or neutron stars (Braithwaite & Spruit 2004; Braithwaite & Nordlund 2006; Braithwaite 2006) and

to theoretical studies of their helicity relaxation (Broderick & Narayan 2008; Mastrano & Melatos 2008). The main generalization of Prendergast's work that we achieve here consists in relaxing the incompressible hypothesis in order to take the star's structure into account (see also Woltjer 1960), which differs as a function of its stellar type and of its evolution stage, and in order to derive the minimum energy equilibrium configuration for a given mass and helicity, which are then applied to realistic models of stellar interiors.

Assuming that the Lorentz volumetric force is a perturbation compared with the gravity, we derived the non force-free magnetohydrostatic equilibrium. In this first article, we focus on the barotropic equilibrium states family[1], for which the possible field configurations and the stellar structure are explicitly coupled. These may correspond to the numerical experiments by Braithwaite and collaborators. In this case, the problem reduces to a Grad-Shafranov-like equation (Grad & Rubin 1958; Shafranov 1966; Kutvitskii & Solov'ev 1994), similar to the one intensively used in fusion plasma physics. We then focus on its minimum energy eigenmodes for a given mass and helicity, which are derived and applied to modeling relaxed stellar fossil magnetic fields, which are found to be non force-free. Arguments in favor of the stability of the obtained configurations are finally discussed (Wright 1973; Tayler 1980; Braithwaite 2009; Reisenegger 2009), and we compare their properties with those of relaxed fields obtained in numerical simulations (Braithwaite 2008). The case of general baroclinic equilibrium states will be studied in Paper II (Wright 1969; Moss 1975).

2. The non force-free magneto-hydrostatic equilibrium

In this work, we focus on the magnetic equilibrium of a self-gravitating spherical shell to model fossil fields in stellar interiors. To achieve this goal, we started from

$$0 = -\nabla P - \rho \nabla V + \boldsymbol{F}_{\mathcal{L}}, \text{ where } \boldsymbol{F}_{\mathcal{L}} = \boldsymbol{j} \times \boldsymbol{B}, \tag{1}$$

which must be satisfied in the interior of an infinitely conducting mass of fluid in the presence of a large-scale field, the Poisson equation, $\nabla^2 V = 4\pi G \rho$, and the Maxwell equations, $\nabla \cdot \boldsymbol{B} = 0$ (Maxwell flux) and $\nabla \times \boldsymbol{B} = \mu_0 \boldsymbol{j}$ (Maxwell-Ampère), where P, ρ, and V are the pressure, the density, and the gravitational potential of the considered plasma, $\boldsymbol{B}$ is the magnetic field, and $\boldsymbol{j}$ the associated current, which is given in the classical MHD approximation by the Maxwell-Ampère's equation. Also, μ_0 is the magnetic permeability of the plasma and $\boldsymbol{F}_{\mathcal{L}}$ is the Lorentz force.

2.1. Magnetic-field configuration and the magnetohydrostatic equilibrium

If we only consider the axisymmetric case, where all physical variables are independent of the azimuthal angle (φ), $\boldsymbol{B}(r, \theta)$ can be written in the form

$$\boldsymbol{B} = \frac{1}{r \sin \theta} \nabla \Psi(r, \theta) \times \hat{\boldsymbol{e}}_\varphi + \frac{1}{r \sin \theta} F(r, \theta) \, \hat{\boldsymbol{e}}_\varphi, \tag{2}$$

which does not diverge and Ψ and F are the poloidal flux function and the toroidal potential, (r, θ, φ) the usual spherical coordinates, and $\{\hat{\boldsymbol{e}}_k\}_{k=r,\theta,\varphi}$ their unit-vector basis. Finally, the poloidal

---

[1] Barotropic states are such that their density and pressure gradients are aligned. They can be convectively stable or not, depending on their entropy stratification. We introduce their precise definition in Sect. 2.2.

component of the magnetic field ($\boldsymbol{B}_{\mathrm{P}}$) is such that $\boldsymbol{B}_{\mathrm{P}} \cdot \nabla \Psi = 0$, so it belongs to iso-$\Psi$ surfaces. The magnetohydrostatic equilibrium (Eq. (1)) implies that the poloidal part (in the meridional plane in the axisymmetric case) of the Lorentz force ($\boldsymbol{F}_{\mathcal{L}_{\mathrm{P}}}$) balances the pressure gradient and the gravitational force, which are also purely poloidal vectors, while its toroidal component ($\boldsymbol{F}_{\mathcal{L}_{\mathrm{T}}} = F_{\mathcal{L}_\varphi} \hat{\boldsymbol{e}}_\varphi$) vanishes in the absence of any other force. We thus have

$$\boldsymbol{F}_{\mathcal{L}} = \boldsymbol{F}_{\mathcal{L}_{\mathrm{P}}} + F_{\mathcal{L}_\varphi} \hat{\boldsymbol{e}}_\varphi = \boldsymbol{F}_{\mathcal{L}_{\mathrm{P}}}. \tag{3}$$

Using Eq. (2), we obtain

$$\boldsymbol{F}_{\mathcal{L}_{\mathrm{P}}} = -\frac{1}{\mu_0 r^2 \sin^2 \theta} \left\{ (F \partial_r F + \partial_r \Psi \Delta^* \Psi) \, \hat{\boldsymbol{e}}_{\mathrm{r}} \right.$$
$$\left. + \frac{1}{r} (F \partial_\theta F + \partial_\theta \Psi \Delta^* \Psi) \, \hat{\boldsymbol{e}}_\theta \right\}, \tag{4}$$

with $\partial_x = \partial/\partial x$, and

$$\Delta^* \Psi \equiv \partial_{rr} \Psi + \frac{\sin \theta}{r^2} \partial_\theta \left(\frac{1}{\sin \theta} \partial_\theta \Psi \right) \tag{5}$$

is the usual Grad-Shafranov operator in spherical coordinates. On the other hand, since $F_{\mathcal{L}_\varphi} = 0$, we get $\partial_r \Psi \partial_\theta F - \partial_\theta \Psi \partial_r F = 0$; therefore the non-trivial values for F are obtained by setting

$$F(r, \theta) = F(\Psi). \tag{6}$$

Then, we obtain $F \partial_r F = F \partial_\Psi F \partial_r \Psi$ and $F \partial_\theta F = F \partial_\Psi F \partial_\theta \Psi$, leading to the final expansion of the Lorentz force

$$\boldsymbol{F}_{\mathcal{L}} = \mathcal{A}(r, \theta) \nabla \Psi, \tag{7}$$

where

$$\mathcal{A}(r, \theta) = -\frac{1}{\mu_0 r^2 \sin^2 \theta} (F \partial_\Psi F + \Delta^* \Psi). \tag{8}$$

Therefore, the poloidal component of $\boldsymbol{F}_{\mathcal{L}}$ is nonzero a priori, the field being thus non force-free in this case.

This point has to be discussed here. First, Reisenegger (2009) demonstrates that the magnetic field cannot be force-free everywhere in stellar interiors (see the demonstration in appendix A of his paper). In this context, the "force-free" configurations obtained by Broderick & Narayan (2008) verify this theorem because they have current sheets with a non-zero Lorentz force on the stellar surface. Moreover, Shulyak et al. (2007, 2010) show how the atmosphere of a CP star can be the host of a non-zero Lorentz force. Therefore, from now on, we consider the non force-free equilibrium.

If we take the curl of Eq. (1), we get the static vorticity equation

$$-\frac{\nabla \rho \times \nabla P}{\rho^2} = \nabla \times \left(\frac{\boldsymbol{F}_{\mathcal{L}}}{\rho} \right), \tag{9}$$

which governs the balance between the baroclinic torque (left-hand side; see Rieutord (2006) for a detailed description) and the magnetic source term. Then, as emphasized by Mestel (1956), the different structural quantities such as the density, the gravitational potential, and the pressure relax in order to verify Eq. (1) for a given field configuration (see Sweet 1950; Moss 1975; Mathis & Zahn 2005, Sect. 5.). Thus, the choice for Ψ is left free.

2.2. The barotropic equilibrium state family

Magnetic initial configurations are one of the crucial unanswered questions for modeling MHD transport processes in stellar interiors. To examine this question, Braithwaite and collaborators (Braithwaite & Spruit 2004; Braithwaite & Nordlund 2006) studied the relaxation of an initially stochastic field in models of convectively stable stellar radiation zones. The field is found to relax, after several Alfvén times, to a mixed poloidal-toroidal equilibrium configuration, which then diffuses towards the exterior.

We choose here to use an analytical approach to find such field geometries, which are governed at the beginning by the magnetohydrostatic equilibrium. To achieve this aim, we focused in this first article on the particular barotropic equilibrium states (in the hydrodynamic meaning of the term) for which the field configuration is explicitly coupled with the stellar structure, since in this case we have

$$-\frac{\nabla \rho \times \nabla P}{\rho^2} = \nabla \times \left(\frac{F_{\mathcal{L}}}{\rho}\right) = \mathbf{0}. \tag{10}$$

Those are the generalizations of the Prendergast's equilibria that take the compressibility into account and that have been studied in polytropic cases by Woltjer (1960), Wentzel (1961), Roxburgh (1966), and Monaghan (1976).

Let us first recall the definition of the barotropic states. In fluid mechanics, a fluid is said to be in a barotropic state if the following condition is satisfied (see Pedlosky (1998) in a geophysical context and Zahn (1992) in a stellar one):

$$\nabla \rho \times \nabla P = \mathbf{0}; \tag{11}$$

in other words, the baroclinic torque in the vorticity equation (Eq. (9)) vanishes. Then, the surfaces of equal density coincide with the isobars since the density and the pressure gradients are aligned. This does not imply any question of equation of state, which in stellar interiors can take the most general form $P = f(\rho, T, \cdots)$ (T being the temperature). Moreover, this does not presume anything about the stratification of the fluid, which can be stably stratified or not. For example, a star in solid body rotation is in a barotropic state (as opposed to baroclinic) (see once again Zahn 1992). Let us illustrate this point with the simplest case of a non-rotating and non-magnetic stellar radiation zone. In this case, the hydrostatic balance is given by $\nabla P/\rho = -\nabla V = \mathbf{g}$. If we take the curl of this equation, we obtain the stationary version of the thermal-wind equation,

$$-\frac{\nabla \rho \times \nabla P}{\rho^2} = -\nabla \times [\nabla V] = \mathbf{0}, \tag{12}$$

and the star is thus in a barotropic state in the hydrodynamic meaning of the term.

This has to be distinguished from the point of view of thermodynamics where a barotropic equation of state is such that $P = f(\rho)$ while a non-barotropic equation of state is such that $P = f(\rho, T, \cdots)$.

Then, it is clear that a fluid with a barotropic equation of state is automatically in a hydrodynamical barotropic state; however, in the case of a fluid with a non-barotropic equation of state, the situation is more subtle. In the case where the curl of the volumetric perturbing force vanishes (i.e. $\nabla \times (F_{\mathcal{L}}/\rho) = 0$), the fluid is in a hydrodynamical barotropic state, while in the general case, it is in a baroclinic situation. Then, a fluid with a non-barotropic equation of state can be in a barotropic state even if it is only for a specific form of the perturbing force. In this first work,

we chose to examine the first equilibrium family in which the Lorentz force verify the barotropic balance described by Eq. (11) in a stably stratified radiation zone. The second general case (cf. Mestel 1956) will be studied in Paper II.

Except just under the surface, stellar interiors are in a regime where $\beta = P/P_{\text{Mag}} \gg 1$, $P_{\text{Mag}} = B^2/(2\mu_0)$ being the plasma's magnetic pressure. On the other hand, in the domain of fields amplitudes relevant for classical stars (i.e. the non-compact objects), the ratio of the volumetric Lorentz force by the gravity is very weak. Therefore, the stellar structure modifications induced by the field can be considered as perturbations only from a spherically symmetric background (Haskell et al. 2008). Then, we can write $\rho \approx \overline{\rho} + \widetilde{\rho}$, where $\overline{\rho}$ and $\widetilde{\rho}$ are, respectively, the mean density on an isobar, which is given at the first order by the standard non-magnetic radial density profile of the considered star, and its magnetic-induced perturbation on the isobar (with $\widetilde{\rho} \ll \overline{\rho}$). Thus to the first order, Eq. (10) on an isobar becomes

$$-\frac{\nabla \widetilde{\rho} \times \mathbf{g}_{\text{eff}}}{\overline{\rho}} = \nabla \times \left(\frac{F_{\mathcal{L}}}{\overline{\rho}}\right) = \mathbf{0}, \tag{13}$$

where the effective gravity ($\mathbf{g}_{\text{eff}}$), such that $\nabla \overline{P} = \overline{\rho}\, \mathbf{g}_{\text{eff}}$, has been introduced. Using Eq. (7), this gives

$$\nabla \left(\frac{\mathcal{A}}{\overline{\rho}}\right) \times \nabla \Psi = \mathbf{0}, \tag{14}$$

which projects only along $\hat{\mathbf{e}}_\varphi$ as

$$\partial_r \left(\frac{\mathcal{A}}{\overline{\rho}}\right)\partial_\theta \Psi - \partial_\theta \left(\frac{\mathcal{A}}{\overline{\rho}}\right)\partial_r \Psi = 0, \tag{15}$$

so that there exists a function G of Ψ such that

$$\frac{\mathcal{A}}{\overline{\rho}} = G(\Psi). \tag{16}$$

Then, Eq. (8) leads to the following one ruling Ψ

$$\Delta^* \Psi + F(\Psi)\,\partial_\Psi [F(\Psi)] = -\mu_0 r^2 \sin^2 \theta\, \overline{\rho}\, G(\Psi). \tag{17}$$

This equation is similar to the well-known Grad-Shafranov equation[2], which is used to find equilibria in magnetically confined plasmas such as those in tokamaks or in spheromaks (Grad & Rubin 1958; Shafranov 1966). However, here the source term is different and is directly related to the internal structure of the star through its density profile ($\overline{\rho}$). The general form of the Grad-Shafranov equation in an astrophysical context is discussed for example in Heinemann & Olbert (1978) and Ogilvie (1997). Moreover, since the field has to be non force-free in stellar interiors $G \neq 0$ (see the previous discussion in Sect. 2.1. and Eqs. (16), (7), and (8)).

It is only applicable to the case of the barotropic state family. The equations for the general case will be studied in Paper II.

2.3. F and G expansion

Let us now focus on the respective expansion of F and G as a function of Ψ. First, since F is a regular function, we can expand it in power series in Ψ:

$$F(\Psi) = \sum_{i=0}^{\infty} \frac{\lambda_i}{R} \Psi^i, \tag{18}$$

---

[2] The usual Grad-Shafranov equation is given by $\Delta^* \Psi + F(\Psi)\,\partial_\Psi [F(\Psi)] = -\mu_0 r^2 \sin^2 \theta \partial_\Psi [P(\Psi)]$, where the pressure P is prescribed in function of Ψ. This only describes the equilibrium between the magnetic force and the pressure gradient.

with λ_i the expansion coefficients that have to be determined, and R a characteristic radius identified below. On the other hand, B_φ must be regular at the center of the sphere. The first term ($i = 0$) of the previous expansion is then excluded (cf. Eq. (2)), the above expansion thus reducing to $F(\Psi) = \sum_{i>0} (\lambda_i/R) \Psi^i$.

In the same way, G can be expanded as

$$G(\Psi) = \sum_{j=0}^{\infty} \beta_j \Psi^j. \tag{19}$$

Then, Eq. (17) becomes

$$\Delta^* \Psi + \sum_{k>0} \frac{\Lambda_k}{R^2} \Psi^k = -\mu_0 r^2 \sin^2 \theta \, \overline{\rho} \sum_{j=0}^{\infty} \beta_j \Psi^j, \tag{20}$$

where $\Lambda_k = \sum_{i_1>0} \sum_{i_2>0} \{i_2 \lambda_{i_1} \lambda_{i_2} \delta_{i_1+i_2-1,k}\}$, with δ the usual Kronecker symbol. This is the generalization of the Grad-Shafranov-type equation obtained by Prendergast (1956) for the barotropic compressible states.

Thus, having assumed the non force-free barotropic magneto-hydrostatic equilibrium state leads to undetermined arbitrary functions (F and G) that must be constrained. To achieve this aim, we follow the method given in the axisymmetric case by Chandrasekhar & Prendergast (1958) and Woltjer (1959b), which allows finding the equilibrium state of lowest energy compatible with the constancy of given invariants for the studied axisymmetric system.

3. Self-gravitating relaxation states

3.1. Definitions and axisymmetric invariants

We first introduce the cylindrical coordinates (s, φ, z) where $s = r \sin \theta$ and $z = r \cos \theta$. Then, $\boldsymbol{B}$ given in Eq. (2) becomes

$$\boldsymbol{B}(s, z) = \frac{1}{s} \boldsymbol{\nabla} \Psi(s, z) \times \hat{\boldsymbol{e}}_\varphi + \frac{1}{s} F(s, z) \, \hat{\boldsymbol{e}}_\varphi. \tag{21}$$

Then, we define the potential vector $\boldsymbol{A}(s, z) = A_\varphi(s, z) \hat{\boldsymbol{e}}_\varphi$, such that $\boldsymbol{B}_{\rm P} = \boldsymbol{\nabla} \times \boldsymbol{A}$ and we get

$$\boldsymbol{B} = \boldsymbol{\nabla} \times \boldsymbol{A} + \frac{F}{s} \hat{\boldsymbol{e}}_\varphi \quad \text{where} \quad A_\varphi(s, z) = \frac{\Psi}{s}. \tag{22}$$

Next, we insert the expansion for the magnetic field $\boldsymbol{B}$ used by Chandrasekhar & Prendergast (1958) and Woltjer (1959a,b):

$$\boldsymbol{B} = -s \, \partial_z \Phi(s, z) \, \hat{\boldsymbol{e}}_s + \frac{1}{s} \partial_s \left[s^2 \Phi(s, z) \right] \hat{\boldsymbol{e}}_z + s \, \mathcal{T}(s, z) \, \hat{\boldsymbol{e}}_\varphi \tag{23}$$

where $\{\hat{\boldsymbol{e}}_k\}_{k=s,\varphi,z}$ is the cylindrical unit-vector basis and where we identify using Eq. (21)

$$\Psi = s^2 \Phi \quad \text{and} \quad F = s^2 \mathcal{T}. \tag{24}$$

The Grad-Shafranov operator applied to Ψ can then be expressed as

$$\Delta^* \Psi = s^2 \, \boldsymbol{\nabla} \cdot \left(\frac{\boldsymbol{\nabla} \Psi}{s^2} \right) = \left[\partial_{ss} - \frac{1}{s} \partial_s + \partial_{zz} \right] \Psi = s^2 \Delta_5 \Phi, \tag{25}$$

where $\Delta_5 = \partial_{ss} + \frac{3}{s} \partial_s + \partial_{zz}$.

We now introduce the two general families of invariants of the barotropic axisymmetric magneto-hydrostatic equilibrium states, which were introduced by Woltjer (1959b) for the compressible case (see also Wentzel 1960):

$$\mathcal{I}_{\mathrm{I};n} = \int_{\mathcal{V}} M_n \left(s^2 \Phi \right) \overline{\rho} \, \mathrm{d}\mathcal{V} = \int_{\mathcal{V}} \left(s^2 \Phi \right)^n \overline{\rho} \, \mathrm{d}\mathcal{V}, \tag{26}$$
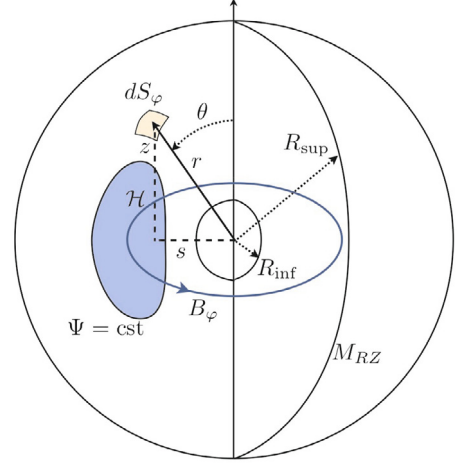
Fig. 1. Schematic representation of the two coordinate systems used and of a constant Ψ surface. The invariants of the axisymmetric system are the total mass of the considered stellar radiative region ($M_{\rm RZ}$), the mass enclosed in a constant Ψ surface, the toroidal flux ($\mathcal{F}_\varphi$) associated with the toroidal magnetic field (B_φ), and the global helicity ($\mathcal{H}$).

$$\mathcal{I}_{\mathrm{II};q} = \int_{\mathcal{V}} N_q \left(s^2 \Phi \right) \mathcal{T} \, \mathrm{d}\mathcal{V} = \int_{\mathcal{V}} \left(s^2 \Phi \right)^q \mathcal{T} \, \mathrm{d}\mathcal{V}, \tag{27}$$

where M_n and N_q are arbitrary functions that have to be specified. They are conserved as long as

$$\boldsymbol{B} \cdot \widehat{\boldsymbol{e}_r} = 0 \quad (\text{i.e. } \Phi = \mathcal{T} = 0) \tag{28}$$

on the boundaries.

3.2. Fossil fields barotropic relaxation states

Let us first concentrate on $\mathcal{I}_{\mathrm{II};q}$ and N_q, which are relevant to fossil fields relaxation. First, if we set $N_0 \left(s^2 \Phi \right) = 1$, we obtain

$$
\begin{aligned}
\mathcal{I}_{\mathrm{II};0} &= \int_{\mathcal{V}} \mathcal{T} \, \mathrm{d}\mathcal{V} = 2\pi \int_{\mathcal{S}} B_\varphi \mathrm{d}s \mathrm{d}z \\
&= 2\pi \int_{\mathcal{S}} B_\varphi \, \mathrm{d}\mathcal{S}_\varphi = 2\pi \mathcal{F}_\varphi,
\end{aligned} \tag{29}
$$

which corresponds to the conservation of the flux of the azimuthal field across the meridional plane of the star ($\mathcal{F}_\varphi$) in perfect axisymmetric MHD equilibria. Then, if we set $N_1 \left(s^2 \Phi \right) = s^2 \Phi$, we get

$$\mathcal{I}_{\mathrm{II};1} = \int_{\mathcal{V}} \left(s^2 \Phi \right) \mathcal{T} \, \mathrm{d}\mathcal{V} = \int_{\mathcal{V}} A_\varphi B_\varphi \mathrm{d}\mathcal{V} = \mathcal{H}/2, \tag{30}$$

where we thus identify the magnetic helicity ($\mathcal{H}$; see Sect. 5.1.) of the field configuration, which is a global quantity integrated over the volume of the studied radiation zone.

Let us briefly discuss the peculiar role of this quantity in the search for stable equilibria. As emphasized by Spruit (2008), the magnetic helicity is a conserved quantity in a perfectly conducting fluid with fixed boundary conditions. However, in realistic conditions, rapid reconnection can take place even at very high conductivity, especially when the field is dynamically evolving, for example, during its initial relaxation phase. Nevertheless, in laboratory experiments, such as in spheromaks, the helicity is often observed to be approximately conserved, which leads to

stable equilibrium configurations. In fact, if the helicity is conserved, a dynamical or unstable field with a finite initial helicity ($\mathcal{H}_0$) cannot decay completely, the helicity of vanishing field being zero. This is precisely what has been observed in the numerical experiment performed by Braithwaite & Spruit (2004) and Braithwaite & Nordlund (2006), where an initial stochastic field with a finite helicity decays initially but relaxes into a stable equilibrium.

In the context of laboratory low-β plasmas, this process has been identified by Taylor (1974) and is thus called the Taylor's relaxation.

For this reason, we now follow Chandrasekhar & Prendergast (1958) to search for the *final state of equilibrium*, which is the state of lowest energy that the compressible star, preserving its axisymmetry, can attain while conserving the invariants $\mathcal{I}_{I;n}$, $\mathcal{I}_{II;0} = \mathcal{F}_\varphi$, and $\mathcal{I}_{II;1} = \mathcal{H}/2$ in barotropic states. To achieve this, we thus introduce the total energy of the system

$$
\begin{aligned}
E &= \frac{1}{2} \int_\mathcal{V} \left\{ \frac{\boldsymbol{B}^2}{\mu_0} + \rho \left[V + 2\mathcal{U} \right] \right\} \mathrm{d}\mathcal{V} \\
&= \frac{1}{2} \int_\mathcal{V} \left\{ \frac{1}{\mu_0} \left[-s^2 \Phi \Delta_5 \Phi + s^2 \mathcal{T}^2 \right] + \rho \left[V + 2\mathcal{U} \right] \right\} \mathrm{d}\mathcal{V},
\end{aligned}
\tag{31}
$$

where $\mathcal{U}$ is the specific internal energy per unit mass (Woltjer 1958, 1959b; Broderick & Narayan 2008). To obtain the minimal energy equilibrium state for the given invariants $\mathcal{I}_{I;n}$ and a given helicity and azimuthal flux, we thus minimize E with respect to $\mathcal{I}_{I;n}$, $\mathcal{I}_{II;0}$, and $\mathcal{I}_{II;1}$. After introducing the associated Lagrangian multipliers ($a_{I;n}, a_{II;0}, a_{II;1}$), this leads to the following condition for a stationary energy:

$$
\delta E + \sum_n a_{I;n} \, \delta \mathcal{I}_{I;n} + \sum_{q=0}^1 a_{II;q} \, \delta \mathcal{I}_{II;q} = 0.
\tag{32}
$$

Following the method described in Chandrasekhar & Prendergast (1958) and Woltjer (1959b), we express δE and $\delta I_{J;r}$ as functions of $\delta \Phi$, $\delta \mathcal{T}$, and $\delta \rho$. Since these variations are independent and arbitrary, their coefficients in the integrand of Eq. (32) must separately vanish, which gives

$$
\begin{aligned}
\frac{1}{\mu_0} \Delta_5 \Phi &= \overline{\rho} \sum_n a_{I;n} \frac{\mathrm{d} M_n \left(s^2 \Phi \right)}{\mathrm{d} \left(s^2 \Phi \right)} + \sum_{q=0}^1 a_{II;q} \mathcal{T} \frac{\mathrm{d} N_q \left(s^2 \Phi \right)}{\mathrm{d} \left(s^2 \Phi \right)} \\
&= \overline{\rho} \sum_n a_{I;n} \frac{\mathrm{d} M_n \left(s^2 \Phi \right)}{\mathrm{d} \left(s^2 \Phi \right)} + a_{II;1} \mathcal{T},
\end{aligned}
\tag{33}
$$

$$
\frac{1}{\mu_0} s^2 \mathcal{T} = -\sum_{q=0}^1 a_{II;q} N_q \left(s^2 \Phi \right) = -a_{II;0} - a_{II;1} s^2 \Phi.
\tag{34}
$$

These equations thus describe the minimal non force-free energy equilibrium states for a given helicity and azimuthal flux. From Eq. (17), we identify that $F(\Psi)$ is now constrained, while $G(\Psi)$, which is required to ensure the non force-free character of the field, is still arbitrary.

Let us now consider the first invariants family ($\mathcal{I}_1$) given in Eq. (26), which are thus needed to constrain $G(\Psi)$. First, the non-magnetic global quantity, which is an invariant of the considered equilibrium, is the total mass of the stellar radiation zone M_{RZ}. We thus set $M_0 \left(s^2 \Phi \right) = 1$, leading naturally to consider the mass

$$
\mathcal{I}_{I;0} = \int_\mathcal{V} \overline{\rho} \, \mathrm{d}\mathcal{V} = M_{RZ}.
\tag{35}
$$

However, since $\mathrm{d} M_0 \left(s^2 \Phi \right) / \mathrm{d} \left(s^2 \Phi \right) = 0$, we thus have to consider the highest order invariant

$$
\mathcal{I}_{I;1} = \int_\mathcal{V} \left(s^2 \Phi \right) \overline{\rho} \, \mathrm{d}\mathcal{V}
\tag{36}
$$

because of the non force-free behavior of the field. This last invariant has been introduced by Prendergast (1956) in the axisymmetric non force-free magneto-hydrostatic incompressible equilibrium, and it corresponds to the mass conservation in each flux tube described by the closed magnetic surface $s^2 \Phi = \mathrm{c}^{\mathrm{ste}}$.

Furthermore, the considered radiation zone is stably stratified. Since in stellar interiors the magnetic pressure is much less than the thermal one, the Lorentz force only has a negligible effect on the gas pressure ($\beta \gg 1$). Moreover, energy is required to move fluid elements in the radial direction because work has to be done against the buoyant restoring force that is thus very strong compared to the magnetic one. Therefore, the radial component of the displacement ($\boldsymbol{\xi}$), which takes place during the adjustment to equilibrium is inhibited $\boldsymbol{\xi} \cdot \widehat{\boldsymbol{e}_r} \approx 0$, and $\boldsymbol{\nabla} \cdot (\overline{\rho} \boldsymbol{\xi}) \approx 0$ due to the anelastic approximation justified in stellar radiation regions. Therefore, as emphasized by Braithwaite (2008), the mass transport in the radial direction is frozen (no matter can leave or enter in the flux tube), and $\mathcal{I}_{I;1}$ can be used as a supplementary constrain in our variational method.

From Eqs. (34)−(34), we thus get the following equations describing the barotropic axisymmetric equilibrium state of lowest energy that the compressible star can reach while conserving its radiation zone mass ($\mathcal{I}_{I;0} = M_{RZ}$), the mass in each flux tube ($\mathcal{I}_{I;1}$), the flux of the toroidal field ($\mathcal{I}_{II;0} = \mathcal{F}_\varphi$), and a given helicity ($\mathcal{I}_{II;1} = \mathcal{H}/2$):

$$
\frac{1}{\mu_0} \Delta_5 \Phi = a_{I;1} \, \overline{\rho} + a_{II;1} \, \mathcal{T},
\tag{37}
$$

$$
\frac{1}{\mu_0} \mathcal{T} = -a_{II;1} \Phi - \frac{a_{II;0}}{s^2}.
\tag{38}
$$

Since the azimuthal field is regular at the origin, we get $a_{II;0} = 0$ from Eq. (23). By eliminating $\mathcal{T}$ between Eqs. (37)−(38), we obtain

$$
\Delta_5 \Phi + \left[\mu_0 a_{II;1} \right]^2 \Phi = \mu_0 \, a_{I;1} \, \overline{\rho},
\tag{39}
$$

which becomes, when multiplying it by s^2 and using Eqs. (24) and (25)

$$
\Delta^* \Psi + \left[\mu_0 a_{II;1} \right]^2 \Psi = \mu_0 \, a_{I;1} \, \overline{\rho} \, r^2 \sin^2 \theta.
\tag{40}
$$

We thus identify in Eq. (20)

$$
\begin{cases} k = 1 \\ j = 0 \end{cases} \quad \text{and} \quad \begin{cases} a_{I;1} = -\beta_0 \\ a_{II;1} = -\frac{1}{\mu_0} \lambda_1 / R, \end{cases}
\tag{41}
$$

where we have constrained the initial arbitrary functions of the magnetohydrostatic equilibrium

$$
F(\Psi) = -\mu_0 a_{II;1} \Psi \quad \text{and} \quad G(\Psi) = -a_{I;1}.
\tag{42}
$$

It then reduces to

$$
\Delta^* \Psi + \frac{\lambda_1^2}{R^2} \Psi = -\mu_0 \overline{\rho} \, r^2 \sin^2 \theta \beta_0,
\tag{43}
$$

with the values of the real coefficients λ_1 and β_0 thus controled by the helicity ($\mathcal{H}$) and the mass conservation in each axisymmetric flux tube defined by $\Psi = \mathrm{c}^{\mathrm{ste}}$ because of the non force-free stably stratified behavior of the reached equilibrium.

As already emphasized, this corresponds to the lowest energy equilibrium state for a given helicity (Bellan 2000; Broderick & Narayan 2008). The equilibrium state ruled by Eq. (43) is thus the generalization of the Taylor relaxation states in a self-gravitating star where the field is not force-free (i.e. $\nabla \times \boldsymbol{B} \neq \alpha \boldsymbol{B}$). Some non force-free relaxed states have been identified in plasma physics (Montgomery & Phillips 1988, 1989; Dasgupta et al. 2002; Shaikh et al. 2008) and should be studied in a stellar context in a near future.

In the case where $\mathcal{I}_{I;1}$ is not considered ($a_{I;1} = \beta_0 = 0$), we recover the Chandrasekhar (1956a) force-free limit (see also Marsh 1992, for a generalization of the solutions) and the usual Taylor's states for low-β plasmas. The Prendergast model is recovered by assuming a constant density profile (incompressible).

3.3. Green's function solution

We are now ready to solve Eq. (43). If we introduce $x = \cos\theta$ and if we set $\mathcal{S}(r,\theta) = -\mu_0 \beta_0 \overline{\rho}\, r^2 \sin^2\theta$, it is recast as

$$\mathcal{L}_{\lambda_1}\Psi = \mathcal{S}, \tag{44}$$

where

$$\mathcal{L}_{\lambda_1} \equiv \left[\partial_{rr} + \frac{1-x^2}{r^2}\partial_{xx} + \frac{\lambda_1^2}{R^2}\right]. \tag{45}$$

Using Green's function method (Morse & Feshbach 1953), we then obtain the particular solution associated with $\mathcal{S}$:

$$\Psi_{\mathrm{p}}(r,x) = -\mu_0 \beta_0 \sum_l \frac{\lambda_1^l}{R_{\mathrm{sup}}}\left[\frac{2l+3}{2(l+1)(l+2)}\right]$$

$$\times \left\{ r\, j_{l+1}\left(\lambda_1^l \frac{r}{R_{\mathrm{sup}}}\right)\int_r^{R_{\mathrm{sup}}}\left[\xi\, y_{l+1}\left(\lambda_1^l \frac{\xi}{R_{\mathrm{sup}}}\right)\mathcal{J}_l(\xi)\right]\mathrm{d}\xi \right.$$

$$\left. + r\, y_{l+1}\left(\lambda_1^l \frac{r}{R_{\mathrm{sup}}}\right)\int_{R_{\mathrm{inf}}}^r \left[\xi\, j_{l+1}\left(\lambda_1^l \frac{\xi}{R_{\mathrm{sup}}}\right)\mathcal{J}_l(\xi)\right]\mathrm{d}\xi \right\}$$

$$\times \left(1-x^2\right)C_l^{3/2}(x), \tag{46}$$

where

$$\mathcal{J}_l(\xi) = \int_{-1}^1 \mathcal{S}(\xi,x')\,C_l^{3/2}(x')\,\mathrm{d}x', \tag{47}$$

and j_l and y_l are respectively the spherical Bessel functions of the first and the second kinds (also called Neumann functions), while $C_l^{3/2}$ are the Gegenbauer polynomials (Abramowitz & Stegun 1972). The variables R_{inf} and R_{sup}, which are respectively the bottom and the top radii of the considered radiation zone, are introduced, and we identify $R = R_{\mathrm{sup}}$.

These functions (j_l, y_l, and $C_l^{3/2}$) are respectively the radial and the latitudinal eigenfunctions of the homogeneous equation associated with Eq. (44):

$$\mathcal{L}_{\lambda_1}\Psi_{\mathrm{h}} = 0. \tag{48}$$

Then, if we express the solutions of this equation as $\Psi_{\mathrm{h}} = \sum_l f_l(r)\,g_l(\theta)$, we get

$$\left(1-x^2\right)\frac{\mathrm{d}^2 g_l}{\mathrm{d}x^2} + (l+1)(l+2)\,g_l = 0 \tag{49}$$

and

$$\frac{\mathrm{d}^2 f_l}{\mathrm{d}r^2} + \left[\left(\frac{\lambda_1^l}{R_{\mathrm{sup}}}\right)^2 - \frac{(l+1)(l+2)}{r^2}\right]f_l = 0 \tag{50}$$

respectively, giving

$$g_l = \left(1-x^2\right)C_l^{3/2}(x) \tag{51}$$

and

$$f_l = K_1^l\, \lambda_1^l\, \frac{r}{R_{\mathrm{sup}}}\, j_{l+1}\left(\lambda_1^l \frac{r}{R_{\mathrm{sup}}}\right)$$

$$+ K_2^l\, \lambda_1^l\, \frac{r}{R_{\mathrm{sup}}}\, y_{l+1}\left(\lambda_1^l \frac{r}{R_{\mathrm{sup}}}\right), \tag{52}$$

where K_1^l and K_2^l are real constants, and λ_1^l are the eigenvalues that allow verification of boundary conditions discussed hereafter. One has to notice that K_2^l has to vanish in order to preserve the regularity of the solution at the center. Applying this to Eq. (43), we finally obtain the general solution

$$\Psi(r,\theta) = \Psi_{\mathrm{h}} + \Psi_{\mathrm{p}}$$

$$= \sin^2\theta \times \left\{ \sum_{l=0}^{\infty} K_1^l\, \frac{\lambda_1^{l,i}}{R_{\mathrm{sup}}}\, r\, j_{l+1}\left(\lambda_1^{l,i}\frac{r}{R_{\mathrm{sup}}}\right)C_l^{3/2}(\cos\theta) \right.$$

$$-\mu_0\beta_0 \frac{\lambda_1^{0,i}}{R_{\mathrm{sup}}}\, r\, j_1\left(\lambda_1^{0,i}\frac{r}{R_{\mathrm{sup}}}\right)\int_r^{R_{\mathrm{sup}}}\left[y_1\left(\lambda_1^{0,i}\frac{\xi}{R_{\mathrm{sup}}}\right)\overline{\rho}\,\xi^3\right]\mathrm{d}\xi$$

$$\left. -\mu_0\beta_0 \frac{\lambda_1^{0,i}}{R_{\mathrm{sup}}}\, r\, y_1\left(\lambda_1^{0,i}\frac{r}{R_{\mathrm{sup}}}\right)\int_{R_{\mathrm{inf}}}^r\left[j_1\left(\lambda_1^{0,i}\frac{\xi}{R_{\mathrm{sup}}}\right)\overline{\rho}\,\xi^3\right]\mathrm{d}\xi \right\}. \tag{53}$$

This particular solution for the poloidal flux function $\left(\Psi_{\mathrm{p}}\right)$ presents a dipolar geometry, owing to its angular dependence that follows the one from the source term $\mathcal{S} = -\mu_0 \beta_0 \overline{\rho}\, r^2 \sin^2\theta$. After neglecting the density, we end up with the linear homogeneous equation, whose solutions are Chandrasekhar-Kendall functions (Chandrasekhar & Kendall 1957). Moreover, because the source term is only constituted of a dipolar component, all the non-dipolar contributions are force-free according to this model.

The magnetic field is then given for $r \leq R_{\mathrm{sup}}$ by

$$\boldsymbol{B} = \frac{1}{r^2\sin\theta}\partial_\theta\Psi\,\hat{\boldsymbol{e}}_r - \frac{1}{r\sin\theta}\partial_r\Psi\,\hat{\boldsymbol{e}}_\theta + \frac{\lambda_1^{0,i}}{R_{\mathrm{sup}}}\frac{\Psi}{r\sin\theta}\,\hat{\boldsymbol{e}}_\varphi. \tag{54}$$

After a few manipulations, we can then express the current density as

$$\boldsymbol{j}_{\mathrm{P}} = \frac{1}{\mu_0}\nabla \times \boldsymbol{B}_{\mathrm{T}} = \underbrace{\frac{\lambda_1^{0,i}}{\mu_0 R}\boldsymbol{B}_{\mathrm{P}}}_{\text{force}-\text{free}}, \tag{55}$$

$$\boldsymbol{j}_{\mathrm{T}} = \frac{1}{\mu_0}\nabla \times \boldsymbol{B}_{\mathrm{P}} = \underbrace{\frac{\lambda_1^{0,i}}{\mu_0 R}\boldsymbol{B}_{\mathrm{T}}}_{\text{force}-\text{free}} + \underbrace{\beta_0\overline{\rho}\, r\sin\theta\,\hat{\boldsymbol{e}}_\varphi}_{\text{non force}-\text{free}}, \tag{56}$$

where we recognize in the first term of the righthand side the force-free contributions and in the second the non force-free one, fully contained in the toroidal component.

The Lorentz force can, as a matter of fact, be written in the very simple form

$$\boldsymbol{F}_{\mathcal{L}} = \boldsymbol{F}_{\mathcal{L}_{\mathrm{P}}} = \beta_0\overline{\rho}\,\nabla\Psi. \tag{57}$$

3.4. Configurations

The boundary conditions for Ψ that determine possible values for K_1^l and $\lambda_1^{0,i}$ must now be discussed. Two major types of geometry are relevant for large-scale fossil magnetic fields in stellar interiors: initially confined and open configurations.

3.4.1. Initially confined configurations

Let us first concentrate on the simplest mathematical solution in the case of a central radiation zone that initially cancels Ψ both at the center ($R_{\mathrm{inf}} = 0$) and at a given confinement radius ($R_{\mathrm{sup}} = R_c$). Then, if we choose to cancel the K_1^l coefficients for every l, the condition $\Psi(0, \theta) = 0$ is verified, since $\lim_{r \to 0} r\, j_1 \left(\lambda_1^{0,i} \frac{r}{R_{\mathrm{sup}}} \right) = 0$. However, if we look at the magnetic field radial component behavior at the center, it is easily shown, with Eq. (54) that if $K_1^0 = 0$ it is given by $\lim_{r \to 0} r^{-1} j_1 \left(\lambda_1^{0,i} \frac{r}{R_{\mathrm{sup}}} \right)$, which does not cancel so that $B_r(0, \theta) \neq 0 = C \cos\theta$ (where $C \in \mathbb{R}^*$). Therefore, this solution is multivalued, thus physically inadmissible, and $K_1^0 \neq 0$.

Then, we consider the general case of a field initially confined between two radii $R_{\mathrm{inf}} = R_{c_1}$ and $R_{\mathrm{sup}} = R_{c_2}$, owing to the presence of both a convective core and a convective envelope (as it is the case e.g. in A-type stars). We impose $\Psi(R_{c_1}, \theta) = 0$ and $\Psi(R = R_{c_2}, \theta) = 0$, which gives the two independent equations for $l = 0$

$$K_1^0 = \mu_0 \beta_0 \int_{R_{c_1}}^{R_{c_2}} \left[y_1 \left(\lambda_1^{0,i} \frac{\xi}{R_{c_2}} \right) \overline{\rho}\, \xi^3 \right] \mathrm{d}\xi \tag{58}$$

and

$$K_1^0 j_1 \left(\lambda_1^{0,i} \right) = \mu_0 \beta_0 y_1 \left(\lambda_1^{0,i} \right) \int_{R_{c_1}}^{R_{c_2}} \left[j_1 \left(\lambda_1^{0,i} \frac{\xi}{R_{c_2}} \right) \overline{\rho}\, \xi^3 \right] \mathrm{d}\xi. \tag{59}$$

We here focus on the dipolar mode that is known to be the lowest energy per helicity ratio state (cf. Broderick & Narayan 2008). These can be formulated so that one first determines the value of $\lambda_1^{0,i}$ according to

$$j_1 \left(\lambda_1^{0,i} \right) \int_{R_{c_1}}^{R_{c_2}} \left[y_1 \left(\lambda_1^{0,i} \frac{\xi}{R_{c_2}} \right) \overline{\rho}\, \xi^3 \right] \mathrm{d}\xi$$
$$- y_1 \left(\lambda_1^{0,i} \right) \int_{R_{c_1}}^{R_{c_2}} \left[j_1 \left(\lambda_1^{0,i} \frac{\xi}{R_{c_2}} \right) \overline{\rho}\, \xi^3 \right] \mathrm{d}\xi = 0, \tag{60}$$

and next computes K_1^0 following (59).

In the case where there is no convective core, as for example in central radiation zones of late-type stars such as the Sun, Eqs. (59) and (60) must be applied setting $R_{c_1} = 0$.

3.4.2. Open configurations

This corresponds to the fields that match at the stellar surface (at $r = R_*$, R_* being the star's radius) with a potential field as observed now in some cases of early-type stars such as Ap stars. Then, we have $\boldsymbol{B}_{\mathrm{ext}} = \boldsymbol{\nabla} \Phi_{\mathrm{M}}$, with Φ_{M} the associated potential.

In the case studied here, we focus on the first configuration (initially confined) since the search of relaxed solutions for given $\mathcal{I}_{\mathrm{I};0}$, $\mathcal{I}_{\mathrm{I};1}$, $\mathcal{I}_{\mathrm{II};0}$, and $\mathcal{I}_{\mathrm{II};1}$ assumes that $\boldsymbol{B} \cdot \hat{\boldsymbol{e}}_r = 0$ on the stellar radiation zones boundaries. This initial confined configuration will then become open one through Ohmic diffusion as in the Braithwaite and collaborators' scenario.

Table 1. Eigenvalues of the first five equilibria for the two configurations illustrated.

Eigenvalue	Solar case	Ap star case
$\lambda_1^{0,1}$	5.276	4.826
$\lambda_1^{0,2}$	9.157	8.657
$\lambda_1^{0,3}$	12.951	12.444
$\lambda_1^{0,4}$	16.290	16.174
$\lambda_1^{0,5}$	19.839	19.849

4. Application to realistic stellar interiors

To illustrate our purpose, we applied our analytical results (i) to model an initial fossil field buried below the convective envelope of the young Sun on the ZAMS and then (ii) to model an initial field present in the radiation zone of a ZAMS 2.40 $M_\odot$ magnetic Ap-star, whose lower and upper radiation-convection interfaces are located at $R_{c_1} = 0.111\, R_*$ and at $R_{c_2} = 0.992\, R_*$ respectively. In the first case, the parameter β_0 is determined such that the maximum field strength reaches the amplitude of $B_0 = 2.1$ MG, which is one of the upper limits given by Friedland & Gruzinov (2004) for the present Sun's radiative core. In the second case, it is obtained such that it reaches the arbitrary value of $B_0 = 10$ kG. This value has approximatively the same order of magnitude as the mean surface amplitude observed using spectropolarimetry for magnetic Ap-star, which exhibits strong external dipolar magnetic behavior (such as HD12288, Wade et al. 2000). We thus assume that such an initial confined internal field is a potential prelude to the multipolar one now observed at the surface, the latter state being acheived after a diffusive process to be studied in a forthcoming paper.

4.1. Fossil fields buried in late-type stars radiative cores

The young Sun model used as a reference is a CESAM non-rotating standard one (Morel 1997), following input from the work of Couvidat et al. (2003) and Turck-Chièze et al. (2004).

In Fig. 2, three possible configurations for Ψ are given. We chose those corresponding to the first, the third, and the fifth eigenvalues (given in Table 1). Those are the generalization of the well-known Grad-Shafranov equation linear eigenmodes obtained in the force-free case (cf. Marsh 1992). The field is then of mixed-type (B_φ is given for $\lambda_1^{0,1}$), both poloidal and toroidal, and non force-free, properties already obtained by Prendergast (1956) in the incompressible case. The respective amplitudes ratio between the poloidal and the toroidal components are described in Sect. 5., where the possible stability of such configurations are discussed.

4.2. Fossil fields in early-type stars

Respective corresponding possible configurations in the case of an Ap star are given in Fig. 3. The model is typical of an A2p-type star, with an initial mass $M_{\mathrm{A}} = 2.40\, M_\odot$. The solar metallicity is chosen as the initial one, and the model is taken on the ZAMS, its luminosity being $L_* = 38.0\, L_\odot$.

Obtained configurations are then mixed poloidal-toroidal (twisted) fields, which may be stable in stellar radiation zones (cf. Braithwaite & Spruit 2004; Braithwaite & Nordlund 2006). Their configurations are thus given in both cases by concentric torus, the neutral points (where $\partial_r \Psi = \partial_\theta \Psi = 0$ so that $B_r = B_\theta = 0$) being position functions of the internal density profile of the star.
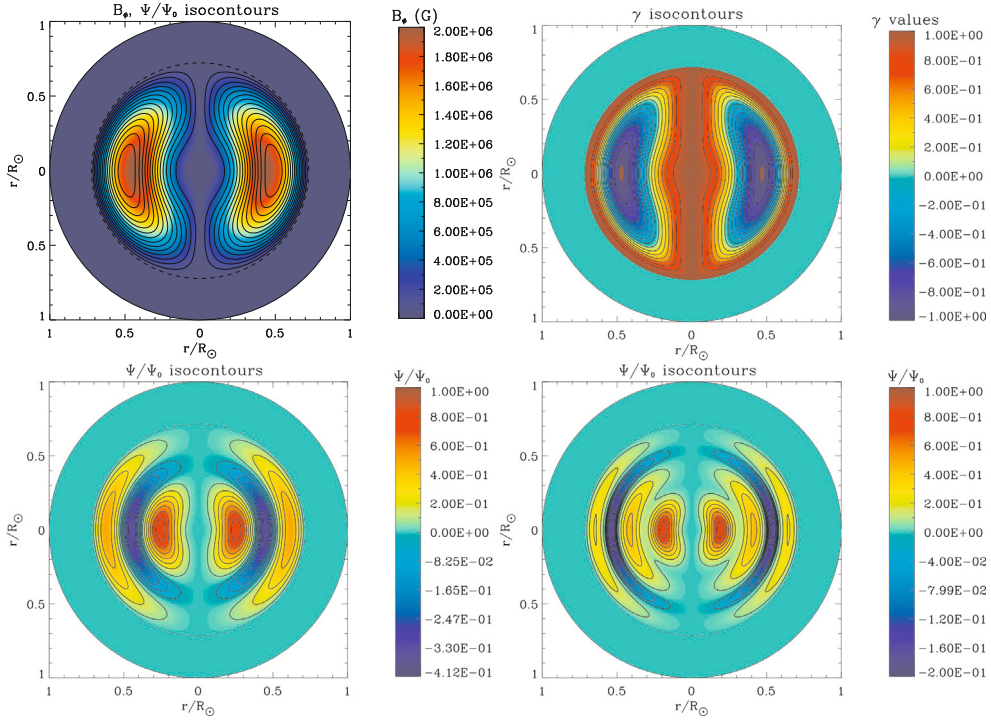
Fig. 2. *Upper panel*: *(left)* toroidal magnetic field strength in colorscale and normalized isocontours of the poloidal flux function Ψ in meridional cut in the solar case where the field is buried in the radiative core (below $0.726R_*$) for the first equilibrium configuration ($\lambda_1^{0,1}$); *(right)* anisotropy factor γ (Eq. (88)). *Lower panel*: normalized isocontours of the flux function Ψ in meridional cut *(left)* for the third possible eigenvalue ($\lambda_1^{0,3}$) in the same case, *(right)* for the fifth possible eigenvalue ($\lambda_1^{0,5}$). The dashed circles indicate the radiation-convection limits.

Let us emphasize here that the original approach of this work first consists in deriving the Grad-Shafranov-like equation adapted to treating the barotropic magnetohydrostatic equilibrium states for realistic models of stellar interiors. Such an approach has already been applied to investigate the internal magnetic configurations in polytropes and in compact objects such as white dwarfs or neutron stars (see e.g. Monaghan 1976; Payne & Melatos 2004; Tomimura & Eriguchi 2005; Yoshida et al. 2006; Haskell et al. 2008; Akgün & Wasserman 2008; Kiuchi & Kotake 2008).

Then, the obtained arbitrary functions are constrained with deriving minimal-energy equilibrium configurations for a given conserved mass, azimuthal flux, and helicity that generalizes the relaxation Taylor's states to the self-gravitating case where the field is non-force free.

5. Links between the field's helicity, topology, and energy

5.1. Helicity vs. mixity

Let us express the magnetic field ($\boldsymbol{B}$) in terms of magnetic stream functions ξ_P (for the poloidal component of the field) and ξ_T (for its toroidal part):

$$\boldsymbol{B} = \boldsymbol{\nabla} \times \left[\boldsymbol{\nabla} \times [\xi_P(r,\theta)\widehat{\boldsymbol{e}}_r] + \xi_T(r,\theta)\widehat{\boldsymbol{e}}_r \right]. \tag{61}$$

Next, the vector potential $\boldsymbol{A}$ is given by the relation $\boldsymbol{B} = \boldsymbol{\nabla} \times \boldsymbol{A}$. Knowing that the gauge choice is inconsequential in the confined case, we can identify without further ado

$$\boldsymbol{A} = \boldsymbol{\nabla} \times [\xi_P(r,\theta)\widehat{\boldsymbol{e}}_r] + \xi_T(r,\theta)\widehat{\boldsymbol{e}}_r. \tag{62}$$

The magnetic stream functions are then projected on the spherical harmonics

$$\xi_P(r,\theta) = \sum_{\ell>0} \xi_0^\ell(r) Y_\ell^0(\theta), \tag{63}$$

$$\xi_T(r,\theta) = \sum_{\ell>0} \chi_0^\ell(r) Y_\ell^0(\theta). \tag{64}$$

From now on, we use Einstein summation convention where $A^\ell B_\ell = \sum_\ell A^\ell B_\ell$ and the vectorial spherical harmonics basis $\left(\boldsymbol{R}_\ell^0(\theta), \boldsymbol{S}_\ell^0(\theta), \boldsymbol{T}_\ell^0(\theta) \right)$ such that any axisymmetric vector field $\boldsymbol{u}(r,\theta)$ can be expanded as

$$\boldsymbol{u}(r,\theta) = u_0^\ell(r)\,\boldsymbol{R}_\ell^0(\theta) + v_0^l(r)\,\boldsymbol{S}_\ell^0(\theta) + w_0^\ell(r)\,\boldsymbol{T}_\ell^0(\theta), \tag{65}$$

where the vectorial spherical harmonics $\boldsymbol{R}_\ell^0(\theta)$, $\boldsymbol{S}_\ell^0(\theta)$, and $\boldsymbol{T}_\ell^0(\theta)$ are defined by

$$\boldsymbol{R}_\ell^0(\theta) = Y_\ell^0(\theta)\,\widehat{\boldsymbol{e}}_r,\ \boldsymbol{S}_\ell^0(\theta) = \boldsymbol{\nabla}_S Y_\ell^0(\theta),\ \boldsymbol{T}_\ell^0(\theta) = \boldsymbol{\nabla}_S \times \boldsymbol{R}_\ell^0(\theta), \tag{66}$$

the horizontal gradient being defined as $\boldsymbol{\nabla}_S = \hat{\boldsymbol{e}}_\theta\,\partial_\theta$ (cf. Rieutord 1987). Since

$$\boldsymbol{\nabla} \times (\xi_P \widehat{\boldsymbol{e}}_r) = \boldsymbol{\nabla} \times \left(\xi_0^\ell Y_\ell^0 \widehat{\boldsymbol{e}}_r \right) = \boldsymbol{\nabla} \times \left(\xi_0^\ell \boldsymbol{R}_\ell^0 \right) = \frac{\xi_0^\ell}{r} \boldsymbol{T}_\ell^0, \tag{67}$$

we get from Eq. (62)

$$\boldsymbol{A} = \chi_0^\ell \boldsymbol{R}_\ell^0 + \frac{\xi_0^\ell}{r} \boldsymbol{T}_\ell^0. \tag{68}$$

On the other hand, we have

$$\boldsymbol{B} = \frac{\ell(\ell+1)}{r^2} \xi_0^\ell \boldsymbol{R}_\ell^0 + \frac{1}{r} \partial_r \xi_0^\ell \boldsymbol{S}_\ell^0 + \frac{\chi_0^\ell}{r} \boldsymbol{T}_\ell^0, \tag{69}$$
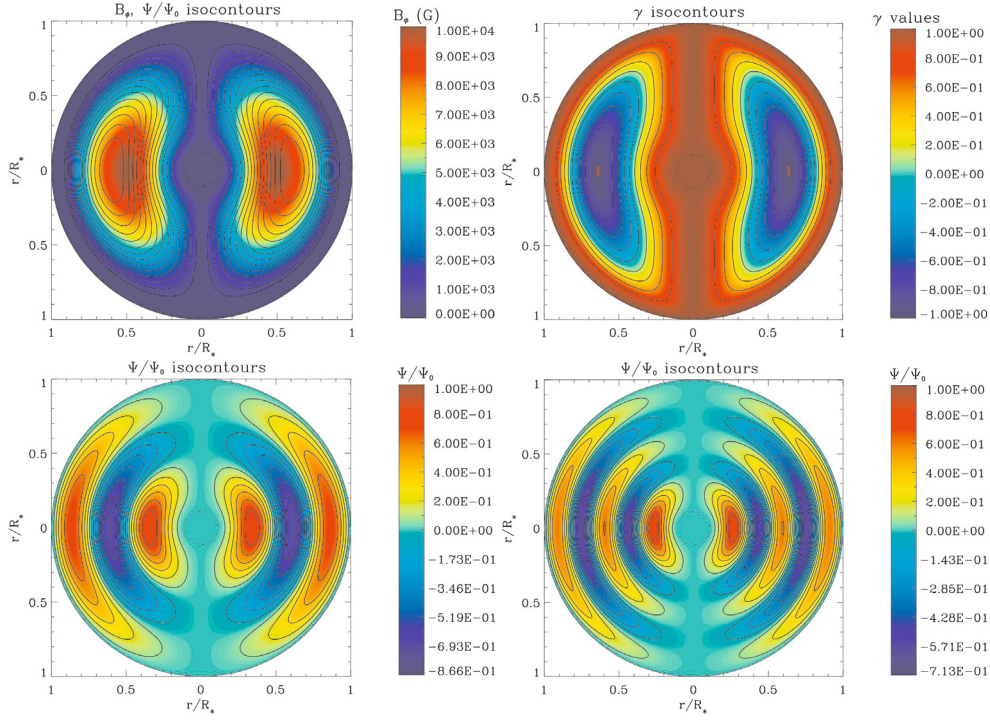
Fig. 3. *Upper panel*: *(left)* toroidal magnetic field strength in colorscale and normalized isocontours of the poloidal flux function Ψ in meridional cut in the Ap star's case where the field is confined between $R_{c_1} = 0.111\,R_*$ and $R_{c_2} = 0.992\,R_*$ for the first equilibrium configuration $(\lambda_1^{0,1})$; *(right)* anisotropy factor γ (Eq. (88)). *Lower panel*: normalized isocontours of the flux function Ψ in meridional cut *(left)* for the third possible eigenvalue $(\lambda_1^{0,3})$ in the same case, *(right)* for the fifth possible eigenvalue $(\lambda_1^{0,5})$. The dashed circles indicate the radiation-convection limits.

from which we finally obtain the expression for the helicity

$$
\mathcal{H} = \int_0^{R_*} \int_\Omega \left\{ \left[\chi_0^\ell \, \boldsymbol{R}_\ell^0 + \frac{\xi_0^\ell}{r} \boldsymbol{T}_\ell^0 \right] \cdot \right. \\
\left. \left[\frac{\ell'\,(\ell'+1)}{r^2} \xi_0^{\ell'} \, \boldsymbol{R}_{\ell'}^0 + \frac{1}{r} \partial_r \xi_0^{\ell'} \, \boldsymbol{S}_{\ell'}^0 + \frac{\chi_0^{\ell'}}{r} \boldsymbol{T}_{\ell'}^0 \right] \right\} \mathrm{d}\Omega \, r^2 \mathrm{d}r. \quad (70)
$$

At this point, we define a "poloidal helicity" defined by

$$
\mathcal{H}_\mathrm{P} = \int_\mathcal{V} \boldsymbol{A}_\mathrm{P} \cdot \boldsymbol{B}_\mathrm{P} \, \mathrm{d}\mathcal{V} \quad (71)
$$

and a "toroidal helicity" by

$$
\mathcal{H}_\mathrm{T} = \int_\mathcal{V} A_\phi B_\phi \, \mathrm{d}\mathcal{V}. \quad (72)
$$

Since $\left(\boldsymbol{R}_\ell^0, \boldsymbol{S}_\ell^0, \boldsymbol{T}_\ell^0 \right)$ constitutes an orthogonal basis,

$$
\int_\Omega \boldsymbol{R}_\ell^0 \cdot \boldsymbol{S}_\ell^0 \mathrm{d}\Omega = \int_\Omega \boldsymbol{R}_\ell^0 \cdot \boldsymbol{T}_\ell^0 \mathrm{d}\Omega = \int_\Omega \boldsymbol{S}_\ell^0 \cdot \boldsymbol{T}_\ell^0 \mathrm{d}\Omega = 0, \quad (73)
$$

we get from the previous expression:

$$
\mathcal{H} = \int_0^{R_*} \left[\frac{\ell'\left(\ell'+1\right)}{r^2} \chi_0^\ell \, \xi_0^{\ell'} \int_\Omega \boldsymbol{R}_\ell^0 \cdot \boldsymbol{R}_{\ell'}^0 \, \mathrm{d}\Omega \right. \\
\left. + \frac{1}{r^2} \xi_0^\ell \chi_0^{\ell'} \int_\Omega \boldsymbol{T}_\ell^0 \cdot \boldsymbol{T}_{\ell'}^0 \, \mathrm{d}\Omega \right] r^2 \mathrm{d}r, \quad (74)
$$

and we verify that

$$
\mathcal{H} = \mathcal{H}_\mathrm{P} + \mathcal{H}_\mathrm{T}. \quad (75)
$$

From this expression (74) we can draw two conclusions:

1. A magnetic field has to be mixed (both poloidal and toroidal) to be helical;
2. The poloidal and the toroidal helicities are equal. This can be verified by exploiting the orthogonality relations

$$
\int_\Omega \boldsymbol{R}_\ell^0 \cdot \boldsymbol{R}_{\ell'}^0 \, \mathrm{d}\Omega = \delta_{\ell,\ell'} \quad (76)
$$

and

$$
\int_\Omega \boldsymbol{T}_\ell^0 \cdot \boldsymbol{T}_{\ell'}^0 \, \mathrm{d}\Omega = \ell\,(\ell+1)\,\delta_{\ell,\ell'}, \quad (77)
$$

where $\delta_{\ell,\ell'}$ is the usual Kronecker symbol. Then, we get

$$
\mathcal{H}_\mathrm{P} = \mathcal{H}_\mathrm{T} = \ell\,(\ell+1) \int_0^{R_*} \xi_0^\ell \chi_0^\ell \, \mathrm{d}r = \mathcal{H}/2. \quad (78)
$$

5.2. Helicity vs. energy

Now, we focus again on the helicity expression in terms of the poloidal flux function Ψ. Equations (55) and (56) are rewritten as

$$
\boldsymbol{B}_\mathrm{P} = \frac{R}{\lambda_1^{0,i}} \boldsymbol{\nabla} \times \boldsymbol{B}_\mathrm{T}, \quad (79)
$$

$$
\boldsymbol{B}_\mathrm{T} = \frac{R}{\lambda_1^{0,i}} \boldsymbol{\nabla} \times \boldsymbol{B}_\mathrm{P} - \frac{R}{\lambda_1^{0,i}} \mu_0 \beta_0 \, \overline{\rho} \, r^2 \, \sin\theta \, \hat{\boldsymbol{e}}_\varphi
$$
$$
= \frac{R}{\lambda_1^{0,i}} \boldsymbol{\nabla} \times \left[\boldsymbol{B}_\mathrm{P} - \mu_0 \beta_0 \, \overline{\rho} \, r^2 \, \cos\theta \, \hat{\boldsymbol{e}}_r \right]. \quad (80)
$$

We thus obtain the two vector potentials

$$
\boldsymbol{A}_\mathrm{P} = \frac{R}{\lambda_1^{0,i}} \left(\boldsymbol{B}_\mathrm{P} - \mu_0 \beta_0 \, \overline{\rho} \, r^2 \, \cos\theta \, \hat{\boldsymbol{e}}_r \right) + \boldsymbol{\nabla}\Lambda_\mathrm{P}, \quad (81)
$$

$$A_{\mathrm{T}} = \frac{R}{\lambda_1^{0,i}} B_{\mathrm{T}} + \nabla \Lambda_{\mathrm{T}}, \tag{82}$$

where Λ_{P} and Λ_{T} are scalar gauge fields left free. When deriving the poloidal and toroidal helicities with the boundary condition $B \cdot \widehat{e}_r = 0$ at the surface, these disappear after integration so we find

$$\mathcal{H}_{\mathrm{P}} = \frac{2\,\mu_0\,R}{\lambda_1^{0,i}} \int_{\mathcal{V}} \frac{B_{\mathrm{P}}^2}{2\,\mu_0} \, \mathrm{d}\mathcal{V} - \frac{\mu_0\,R}{\lambda_1^{0,i}} \beta_0 \int_{\mathcal{V}} \overline{\rho}\,\Psi\,\mathrm{d}\mathcal{V}, \tag{83}$$

$$\mathcal{H}_{\mathrm{T}} = \frac{2\,\mu_0\,R}{\lambda_1^{0,i}} \int_{\mathcal{V}} \frac{B_{\mathrm{T}}^2}{2\,\mu_0} \, \mathrm{d}\mathcal{V}. \tag{84}$$

After, introducing the poloidal and toroidal magnetic energies $U_{\mathrm{mag;P}} = \int_{\mathcal{V}} \frac{B_{\mathrm{P}}^2}{2\mu_0}\,\mathrm{d}\mathcal{V}$ and $U_{\mathrm{mag;T}} = \int_{\mathcal{V}} \frac{B_{\mathrm{T}}^2}{2\mu_0}\,\mathrm{d}\mathcal{V}$ (respectively), we obtain

$$\mathcal{H}_{\mathrm{P}} = \frac{2\,\mu_0\,R}{\lambda_1^{0,i}} \left(U_{\mathrm{mag,P}} - \frac{1}{2}\beta_0 M_\Psi \right), \tag{85}$$

where we identify $M_\Psi = \mathcal{I}_{I;1} = \int_{\mathcal{V}} \overline{\rho}\,\Psi\,\mathrm{d}\mathcal{V}$, and

$$\mathcal{H}_{\mathrm{T}} = \frac{2\,\mu_0\,R}{\lambda_1^{0,i}} U_{\mathrm{mag,T}}. \tag{86}$$

Finally, by adding these two last equations, we get the global relation between the helicity and the magnetic energy in the non force-free case

$$\mathcal{H} = \frac{2\,\mu_0\,R}{\lambda_1^{0,i}} \left(U_{\mathrm{mag}} - \frac{1}{2}\beta_0 M_\Psi \right), \tag{87}$$

where we recognize the non force-free contribution in the second term, which is the first invariant: the mass enclosed in magnetic flux surface.

5.3. Helicity vs. topology

The $l > 1$ latitudinal mode contributions

As shown by Broderick & Narayan (2008) for a set of modes l ranging from 1 to 8 in the case of force-free solutions applied in an incompressible media, the first dipolar eigenvalue $\lambda_1^{0,1}$ corresponds to the minimum energy configuration. Furthermore, from the Eq. (87), it arises directly that adding contributions from the higher multipolar components of the field (force-free) will result in adding a positive amount of magnetic energy to the total energy, and this one will not be the minimal state.

Lowest energy radial mode

We plotted in Figs. 4a and 4b the poloidal, toroidal, and total helicity for the Sun and of the Ap star. It clearly follows from this figure that the poloidal and the toroidal helicities are equal (cf. Eq. (78)) for the eigenvalues given in Table 1. Moreover, the energy of the poloidal component of the field ($U_{\mathrm{mag,P}}$) can be compared to the one correponding to the toroidal part ($U_{\mathrm{mag,T}}$), and we see that they have the same order of magnitude.

Figures 5a and 5b represent the ratios $\mathcal{E}_{\mathrm{mag}}/\mathcal{H}$ for the poloidal, toroidal, and global contributions, with and without the non force-free term, as a function of the parameter $\lambda_1^{0,i}$ in the case of the Sun and of the Ap type star. The first dipolar eigenvalue $\lambda_1^{0,1}$ presents the minimum energy compared with highest radial modes. It is thus the most probable configuration achieved after relaxation, so from now on we focus on it.
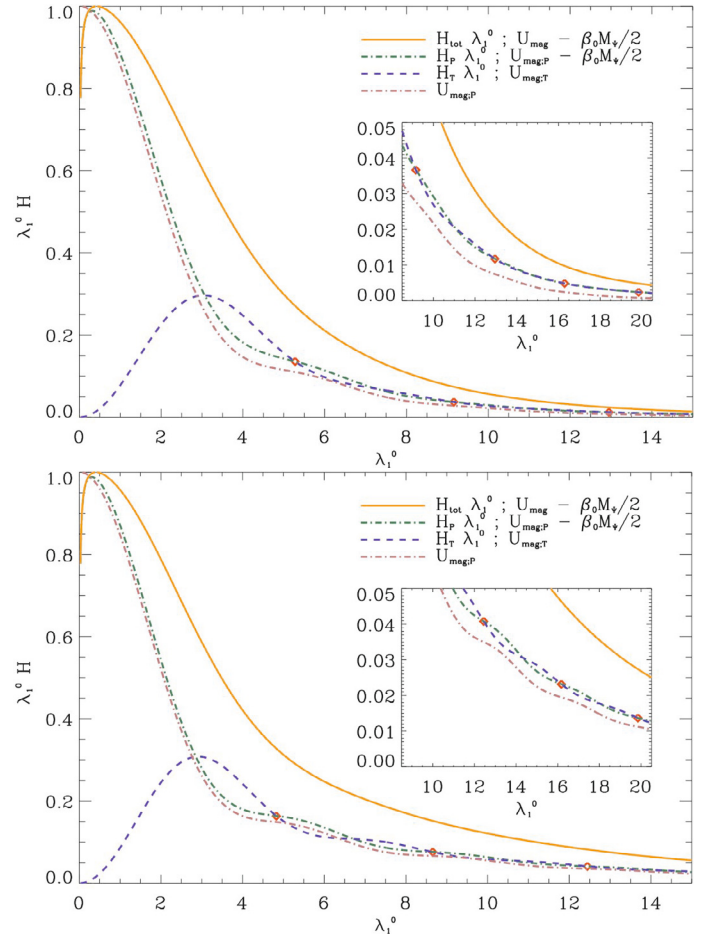
Fig. 4. Normalized total, poloidal, and toroidal helicities as a function of the eigenvalue (λ_1^0) in the case of the young Sun (a, *top*) and of the studied Ap star (b, *bottom*). The red diamonds represent the eigenvalues ($\lambda_1^{0,i}$) given in Table 1 for which Eq. (78) is verified. Using Eq. (86), we directly deduce $U_{\mathrm{mag;T}}$ while $U_{\mathrm{mag;P}}$ is given in purple.

6. Discussion

6.1. Stability criteria

First, it is interesting to examine the ratio of the field's poloidal component amplitude with its toroidal one. Then, we define the anisotropy factor (γ) of the configuration[3] by

$$\gamma(r, \theta) = \frac{B_{\mathrm{P}}^2 - B_{\mathrm{T}}^2}{B_{\mathrm{P}}^2 + B_{\mathrm{T}}^2}, \quad \text{where} \quad B_{\mathrm{P}} = \sqrt{B_r^2 + B_\theta^2}. \tag{88}$$

It runs between -1 when the field is completely toroidal to 1 when it is completely poloidal. In Figs. 2 and 3, it is shown for the first configurations obtained in the solar and in the Ap star cases. In both ones, the field is strongly toroidal ($\gamma \approx -1$) in the center of the torus, which corresponds to the neutral point of the poloidal field (where we recall that $\partial_r \Psi = \partial_\theta \Psi = 0$), while it is strongly poloidal ($\gamma \approx 1$) around the magnetic axis of the star where the toroidal field is weak. Between those two regimes, both components have comparable strengths where $\gamma \approx 0$. Then, proposed configurations may be stable since

---

[3] This can be inverted as $\frac{B_{\mathrm{T}}}{B_{\mathrm{P}}} = \sqrt{\frac{1-\gamma}{1+\gamma}}$ and $\frac{u_{\mathrm{mag,T}}}{u_{\mathrm{mag,P}}} = \frac{1-\gamma}{1+\gamma}$, where the magnetic energy densities associated with the poloidal field ($u_{\mathrm{mag,P}} = B_{\mathrm{P}}^2/2\mu_0$) and with the toroidal one ($u_{\mathrm{mag,T}} = B_{\mathrm{T}}^2/2\mu_0$) have been introduced.
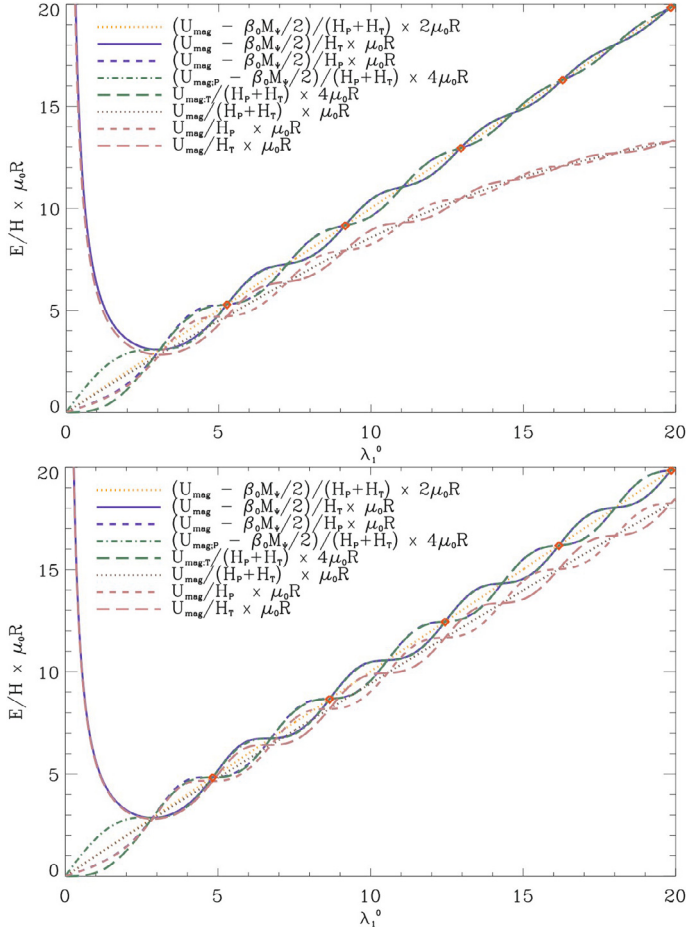
Fig. 5. Magnetic energy/helicity ratios for the total, poloidal, and toroidal contributions as a function of the eigenvalue (λ_1^0) with (first five curves) and without (last three curves) the non-force-free term in the case of the young Sun (a, *top*) and of the studied Ap star (b, *bottom*). For the eigenvalues $(\lambda_1^{0,i})$ represented by the red diamonds (cf. Table 1), Eqs. (78), (87), (85), (86) are simultaneously verified.

poloidal and toroidal fields can stabilize each other (Wright 1973; Tayler 1980; Braithwaite 2009). The complete stability analysis following the analytical method given in Bernstein et al. (1958) and using 3D numerical simulations will be achieved in the near future.

6.2. Comparison to numerical simulations

Next, let us compare our analytical configuration in more details to those obtained using numerical simulations (see Braithwaite & Spruit 2004; Braithwaite & Nordlund 2006; Braithwaite 2008). Braithwaite and collaborators performed numerical magnetohydrodynamical simulations of the relaxation of an initially random magnetic field in a stably stratified star. Then, this initial magnetic field is always found to relax on the Alfvén time scale into a stable magneto-hydrostatic equilibrium mixed configuration consisting of twisted flux tube(s). Two families are then identified: in the first, the equilibria configurations are roughly axisymmetric with one flux tube forming a circle around the equator, such as in our configuration; in the second family, the relaxed fields are non-axisymmetric consisting of one or more flux tubes forming a complex structure with their axis lying at roughly constant depth under the surface of the star. Whether an axisymmetric or non-axisymmetric equilibrium forms depends

on the initial condition chosen for the radial profile of the initial stochastic field strength $||\boldsymbol{B}|| \propto \overline{\rho}^p$: a centrally concentrated one evolves into an axisymmetric equilibrium as in our configuration while a more spread-out field with a stronger connection to the atmosphere relaxes into a non-axisymmetric one. Braithwaite (2008) indicates that, if using an ideal-gas star modeled initially with a polytrope of index $n = 3$, the threshold is $p \approx 1/2$.

Moreover, as shown in Fig. 7 in Braithwaite (2008), a selective decay of the total helicity ($\mathcal{H}$) and of the magnetic energy (U_{Mag}) occurs during the initial relaxation with a stronger decrease in U_{Mag} than that of $\mathcal{H}$. This hierarchy, which is well known in plasma physics (see for example Biskamp 1997; Shaikh et al. 2008) justifies the variational method used to derive our configuration (Montgomery & Phillips 1988) while the introduction of $\mathcal{I}_{\mathrm{I};1}$ is justified by the non force-free character of the field in stellar interiors (Reisenegger 2009) and by the stratification, which inhibits the transport of flux and mass in the radial direction (see Sect. 3.2 and Braithwaite 2008).

Finally, note that our analytical configuration for which $U_{\mathrm{mag;P}}/U_{\mathrm{mag}} \approx 0.45$ verifies the stability criterion derived by Braithwaite (2009) for axisymmetric configurations:

$$\mathcal{A}\frac{U_{\mathrm{mag}}}{U_{\mathrm{grav}}} < \frac{U_{\mathrm{mag,P}}}{U_{\mathrm{mag}}} \le 0.8, \qquad (89)$$

where U_{grav} is the gravitational energy in the star, and $\mathcal{A}$ a dimensionless factor whose value is ∼10 in a main-sequence star and ∼10^3 in a neutron star, while we expect $U_{\mathrm{mag}}/U_{\mathrm{grav}} < 10^{-6}$ in a realistic star (see for example Duez et al. 2010). Our analytical solution is thus similar to the axisymmetric non force-free relaxed solutions family obtained by Braithwaite & Spruit (2004) and Braithwaite & Nordlund (2006).

These types of configurations can thus be relevant to model initial equilibrium conditions for evolutionary calculations involving large-scale fossil fields in stellar radiation zones. First, they can be used to initiate MHD rotational transport in dynamical stellar evolution codes where it is implemented (cf. Mathis & Zahn 2005). There, axisymmetric transport equations have been derived to study the secular dynamics of the mean axisymmetric component of the magnetic field, with the magnetic instabilities treated by using phenomenological prescriptions (Spruit 1999, 2002; Maeder & Meynet 2004) that have to be verified and improved by numerical experiments (Braithwaite 2006; Zahn et al. 2007; Gellert et al. 2008). On the other hand, those can also be used as initial conditions for large-scale numerical simulations of stellar radiation zones (Garaud 2002; Brun & Zahn 2006).

6.3. Relaxed configurations and boundary conditions

Let us now discuss the boundary conditions we chose. Since equilibrium states are known to minimize the energy/helicity ratio, we followed the procedure established by Chandrasekhar & Prendergast (1958) and Woltjer (1959b) for constraining the arbitrary functions of the magnetohydrostatic equilibrium. This procedure, which minimizes the energy with respect to given invariants of the system (and in particular the helicity), assumes the following boundary condition $\boldsymbol{B} \cdot \hat{\boldsymbol{e}}_r = 0$ that leads to an azimuthal current sheet owing the non-zero latitudinal field at the upper boundary ($B_\theta\left(R_{\mathrm{sup}}, \theta\right) \ne 0$). This is a potential source of instability, and in the case of our configuration, we have to evaluate its effect on the stability (cf. Bellan 2000).

Next, in a stellar context, we have to allow open configurations as observed and thus match the internal solution with an external multipolar one. It then remains to be seen whether the

invariants are conserved, as they are in the confined case (Dixon et al. 1989).

Finally, independent of the chosen type of configuration (confined or matched with a multipolar external field), we have to search for solutions that allow the continuity of the magnetic field and of the associated currents at the boundaries to cancel the possible induced instabilities. This leads to an ill-posed problem which must be solved in a subtle way (see Monaghan 1976; Lyutikov 2010). In the present state of art, no solution has been derived that both minimizes the energy/helicity ratio and satisfies this type of surface boundary condition. This will be the next step, but it is beyond the scope of the present paper.

7. Conclusion

In the context of improving stellar models by considering dynamical processes such as rotation and magnetic field, we examined possible magnetic equilibrium configurations to model initial fossil fields.

We generalized the pioneer work by Prendergast (1956) in deriving the barotropic magnetohydrostatic equilibrium states of realistic stellar interiors which are a first equilibrium family. These will then evolve due to other dynamical processes such as Ohmic diffusion, differential rotation, meridional circulation, and turbulence. Relaxed minimum energy equilibrium configurations we then obtained for a given conserved mass and helicity correspond to the Taylor's relaxation states in the self-gravitating non force-free case. These are then applied to the internal radiation zone of the young Sun and to the radiative interior of an Ap star on the ZAMS. Mixed poloidal and toroidal magnetic configurations are obtained, which are potentially stable in stellar radiation zones.

Now, we thus need to study the stability of these magnetic topologies; moreover, the case of general baroclinic equilibrium states has to be studied (Paper II). These equilibrium configurations then have to be used as possible initial conditions for rotational transport processes in those stellar radiative regions that will allow to study internal stellar MHD on secular time scales.

References

Abramowitz, M., & Stegun, I. A. 1972, Handbook of Mathematical Functions (New York: Dover)
Acheson, D. J. 1978, Roy. Soc. Lond. Phil. Trans. Ser. A, 289, 459
Aerts, C., Christensen-Dalsgaard, J., Cunha, M., & Kurtz, D. W. 2008, Sol. Phys., 251, 3
Akgün, T., & Wasserman, I. 2008, MNRAS, 383, 1551
Bellan, P. M. 2000, Spheromaks: a practical application of magnetohydrodynamic dynamos and plasma self-organization (River Edge, NJ: Imperial College Press)
Bernstein, I. B., Frieman, E. A., Kruskal, M. D., & Kulsrud, R. M. 1958, Roy. Soc. Lond. Proc. Ser. A, 244, 17
Biskamp, D. 1997, Nonlinear Magnetohydrodynamics (Cambridge, UK: Cambridge University Press)
Braithwaite, J. 2006, A&A, 449, 451
Braithwaite, J. 2007, A&A, 469, 275
Braithwaite, J. 2008, MNRAS, 386, 1947
Braithwaite, J. 2009, MNRAS, 397, 763
Braithwaite, J., & Nordlund, Å. 2006, A&A, 450, 1077
Braithwaite, J., & Spruit, H. C. 2004, Nature, 431, 819
Broderick, A. E., & Narayan, R. 2008, MNRAS, 383, 943
Brun, A. S., & Zahn, J. P. 2006, A&A, 457, 665
Chandrasekhar, S. 1956a, Proc. Nat. Acad. Sci., 42, 1
Chandrasekhar, S. 1956b, Proc. Nat. Acad. Sci., 42, 273
Chandrasekhar, S., & Kendall, P. C. 1957, ApJ, 126, 457
Chandrasekhar, S. & Prendergast, K. H. 1956, Proc. Nat. Acad. Sci., 42, 5
Chandrasekhar, S., & Prendergast, K. H. 1958, in Electromagnetic Phenomena in Cosmical Physics, ed. B. Lehnert, IAU Symp., 6, 46
Charbonneau, P., & MacGregor, K. B. 1993, ApJ, 417, 762
Couvidat, S., Turck-Chièze, S., & Kosovichev, A. G. 2003, ApJ, 599, 1434
Dasgupta, B., Janaki, M. S., Bhattacharyya, R., et al. 2002, Phys. Rev. E, 65, 046405
Dixon, A. M., Berger, M. A., Priest, E. R., & Browning, P. K. 1989, A&A, 225, 156
Donati, J. F., Semel, M., Carter, B. D., Rees, D. E., & Collier Cameron, A. 1997, MNRAS, 291, 658
Donati, J. F., Howarth, I. D., Jardine, M. M., et al. 2006, MNRAS, 370, 629
Duez, V., Brun, A. S., Mathis, S., Nghiem, P. A. P., & Turck-Chièze, S. 2008, Mem. Soc. Astron. It., 79, 716
Duez, V., Mathis, S., & Turck-Chièze, S. 2010, MNRAS, 402, 271
Ferraro, V. C. A. 1954, ApJ, 119, 407
Friedland, A., & Gruzinov, A. 2004, ApJ, 601, 570
Garaud, P. 2002, MNRAS, 329, 1
Gellert, M., Rüdiger, G., & Elstner, D. 2008, A&A, 479, L33
Goossens, M., & Tayler, R. J. 1980, MNRAS, 193, 833
Goossens, M., & Veugelen, R. 1978, A&A, 70, 277
Goossens, M., Biront, D., & Tayler, R. J. 1981, Ap&SS, 75, 521
Grad, H., & Rubin, H. 1958, in Proc. of the Second United Nations Int. Conf. on the Peaceful Uses of Atomic Energy, IAEA, Geneva, 31, 190
Haskell, B., Samuelsson, L., Glampedakis, K., & Andersson, N. 2008, MNRAS, 385, 531
Heinemann, M., & Olbert, S. 1978, J. Geophys. Res., 83, 2457
Kiuchi, K., & Kotake, K. 2008, MNRAS, 385, 1327
Kutvitskii, V. A., & Solov'ev, L. S. 1994, Sov. J. Exp. Theor. Phys., 78, 456
Landstreet, J. D., Silaj, J., Andretta, V., et al. 2008, A&A, 481, 465
Li, L., Sofia, S., Ventura, P., et al. 2009, ApJS, 182, 584
Li, L. H., Ventura, P., Basu, S., Sofia, S., & Demarque, P. 2006, ApJS, 164, 215
Lydon, T. J., & Sofia, S. 1995, ApJS, 101, 357
Lyutikov, M., 2010, MNRAS, 402, 345
Maeder, A., & Meynet, G. 2000, ARA&A, 38, 143
Maeder, A., & Meynet, G. 2004, A&A, 422, 225
Markey, P., & Tayler, R. J. 1973, MNRAS, 163, 77
Markey, P., & Tayler, R. J. 1974, MNRAS, 168, 505
Marsh, G. E. 1992, Phys. Rev. A, 45, 7520
Mastrano, A., & Melatos, A. 2008, MNRAS, 387, 1735
Mathis, S., & Zahn, J. P. 2005, A&A, 440, 653
Mestel, L. 1956, MNRAS, 116, 324
Mestel, L., & Moss, D. L. 1977, MNRAS, 178, 27
Monaghan, J. J. 1976, Ap&SS, 40, 385
Montgomery, D., & Phillips, L. 1988, Phys. Rev. A, 38, 2953
Montgomery, D., & Phillips, L. 1989, Physica D, 37, 215
Morel, P. 1997, A&AS, 124, 597
Morse, P. M., & Feshbach, H. 1953, Methods of theoretical physics, International Series in Pure and Applied Physics (New York: McGraw-Hill)
Moss, D. L. 1973, MNRAS, 164, 33
Moss, D. L. 1975, MNRAS, 173, 141
Neiner, C. 2007, in Active OB-Stars: Laboratories for Stellar and Circumstellar Physics, ed. A. T. Okazaki, S. P. Owocki, & S. Stefl, ASP Conf. Ser., 361, 91
Ogilvie, G. I. 1997, MNRAS, 288, 63
Payne, D. J. B., & Melatos, A. 2004, MNRAS, 351, 569
Pedlosky, J. 1998, Geophys. fluid dyn., 2nd edn. (Springer)
Petit, P., Dintrans, B., Solanki, S. K., et al. 2008, MNRAS, 388, 80
Prendergast, K. H. 1956, ApJ, 123, 498
Reisenegger, A. 2009, A&A, 499, 557
Rieutord, M. 1987, Geophys. Astrophys. Fluid Dyn., 39, 163
Rieutord, M. 2006, in EAS Publ. Ser. 21, ed. M. Rieutord, & B. Dubrulle, 275–295
Roxburgh, I. W. 1966, MNRAS, 132, 347
Rudiger, G., & Kitchatinov, L. L. 1997, Astron. Nachr., 318, 273
Shafranov, V. D. 1966, Rev. Plasma Phys., 2, 103
Shaikh, D., Dasgupta, B., Zank, G. P., & Hu, Q. 2008, Phys. Plasmas, 15, 012306
Shulyak, D., Valyavin, G., Kochukhov, O., et al. 2007, A&A, 464, 1089
Shulyak, D., Kochukhov, O., Valyavin, G., et al. 2010, A&A, 509, A28
Spruit, H. C. 1999, A&A, 349, 189

Spruit, H. C. 2002, A&A, 381, 923
Spruit, H. C. 2008, in 40 Years of Pulsars: Millisecond Pulsars, Magnetars and More, ed. C. Bassa, Z. Wang, A. Cumming, & V. M. Kaspi, AIP Conf. Ser., 983, 391
Sweet, P. A. 1950, MNRAS, 110, 548
Talon, S. 2008, in EAS Publ. Ser. 32, ed. C. Charbonnel & J.-P. Zahn, 81
Tayler, R. J. 1973, MNRAS, 161, 365
Tayler, R. J. 1980, MNRAS, 191, 151
Taylor, J. B. 1974, Phys. Rev. Lett., 33, 1139
Tomimura, Y., & Eriguchi, Y. 2005, MNRAS, 359, 1117
Turck-Chièze, S., & Talon, S. 2008, Adv. Space Res., 41, 855
Turck-Chièze, S., Couvidat, S., Piau, L., et al. 2004, Phys. Rev. Lett., 93, 211102
Van Assche, W., Goossens, M., & Tayler, R. J. 1982, A&A, 109, 166

Wade, G. A., Kudryavtsev, D., Romanyuk, I. I., Landstreet, J. D., & Mathys, G. 2000, A&A, 355, 1080
Wentzel, D. G. 1960, ApJS, 5, 187
Wentzel, D. G. 1961, ApJ, 133, 170
Woltjer, L. 1958, Proc. Nat. Acad. Sci., 44, 833
Woltjer, L. 1959a, ApJ, 130, 400
Woltjer, L. 1959b, ApJ, 130, 405
Woltjer, L. 1960, ApJ, 131, 227
Wright, G. A. E. 1969, MNRAS, 146, 197
Wright, G. A. E. 1973, MNRAS, 162, 339
Yoshida, S., Yoshida, S., & Eriguchi, Y. 2006, ApJ, 651, 462
Zahn, J. P. 1992, A&A, 265, 115
Zahn, J. P., Brun, A. S., & Mathis, S. 2007, A&A, 474, 145